

****FULL TITLE****
*ASP Conference Series, Vol. **VOLUME**, **YEAR OF PUBLICATION***
****NAMES OF EDITORS****

On the mass distribution of neutron stars in HMXBs

A. van der Meer

*Astronomical Institute “Anton Pannekoek”, University of Amsterdam,
 Kruislaan 403, NL-1098 SJ Amsterdam, Netherlands*

L. Kaper

*Astronomical Institute “Anton Pannekoek”, University of Amsterdam,
 Kruislaan 403, NL-1098 SJ Amsterdam, Netherlands*

M.H van Kerkwijk

*Department of Astronomy and Astrophysics, University of Toronto, 60
 St George Street, Toronto, ON M5S 3H8, Canada*

E.P.J. van den Heuvel

*Astronomical Institute “Anton Pannekoek”, University of Amsterdam,
 Kruislaan 403, NL-1098 SJ Amsterdam, Netherlands*

Abstract. We present the results of a monitoring campaign of three eclipsing high-mass X-ray binaries (HMXBs: SMC X–1, LMC X–4 and Cen X–3). High-resolution VLT/UVES spectra are used to measure the radial velocities of these systems with high accuracy. We show that the subsequent mass determination of the neutron stars in these systems is significantly improved and discuss the implications of this result.

1. Introduction

A neutron star is the compact remnant of a massive star ($M \gtrsim 8 M_{\odot}$) with a central density of 5 to 10 times the density of an atomic nucleus. The global structure of a neutron star depends on the equation of state (EOS) under these extreme conditions, i.e. the relation between pressure and density in the neutron star interior (Lattimer & Prakash 2004). Given an EOS, the equations of hydrostatic equilibrium can be solved resulting in a mass-radius relation for the neutron star and a corresponding maximum neutron-star mass. The “hardness” of the EOS depends e.g. on how many bosons are present in matter of such a high density. As they do not contribute to the fermi pressure, their presence (e.g. Brown & Bethe 1994) will tend to “soften” the EOS. For a soft EOS, one of the astrophysical implications would be that neutron stars cannot have a large mass (e.g. $< 1.55 M_{\odot}$ for the EOS applied by Brown & Bethe (1994)); for a higher mass, the object would collapse into a black hole.

Given the above, the accurate measurement of neutron-star masses is essential for our understanding of the equation of state (EOS) of matter at supra-nuclear densities. Just by finding one neutron star with a mass higher than the

maximum mass allowed by a given EOS proves the invalidity of that EOS. Currently, the most massive neutron star is the X-ray pulsar Vela X-1 (Barziv et al. 2001; Quaintrell et al. 2003) with a mass of $1.86 \pm 0.16 M_{\odot}$. The millisecond radio pulsar J0751+1807 may have an even higher mass: $2.2 \pm 0.2 M_{\odot}$ (Stairs 2004). Both results are in favor of a stiff EOS (see also Srinivasan 2001).

Another issue is the neutron-star mass distribution: the detailed supernova mechanism producing the neutron star is not understood, but it is likely that the many neutrinos that are produced during the formation of the (proto-) neutron star in the center of the collapsing star play an important role (Burrows 2000). Timmes et al. (1996) present model calculations from which they conclude that Type II supernovae (massive, single stars) give a bimodal neutron-star mass distribution, with peaks at 1.28 and $1.73 M_{\odot}$, while Type Ib supernovae (such as produced by stars in binaries, which are stripped of their envelopes) will produce neutron stars within a small range around $1.32 M_{\odot}$. The massive neutron star in Vela X-1 would be consistent with the second peak in this distribution.

Neutron stars are detected either as radio pulsars, single or in a binary with a white dwarf or neutron star companion, or as X-ray sources in binaries with a (normal) low-mass companion star (LMXB) or a high-mass companion (HMXB). Most HMXBs are Be/X-ray binaries, but we focus on the initially more massive systems: high-mass X-ray binaries (HMXBs) consisting of a massive OB supergiant and a neutron star or a black hole (Kaper & Van der Meer, these proceedings). In five of these systems containing an eclipsing X-ray pulsar the mass of the neutron star has been determined. The masses of all but one (Vela X-1) are consistent with being equal to $1.4 M_{\odot}$. However, most spectroscopic observations used for these mass determinations were carried out more than 20 years ago, before the advent of sensitive CCD detectors and 8m-class telescopes; therefore, the uncertainties are too large to measure a significant mass difference (see Van Kerkwijk et al. 1995).

2. Observations

Here we present new, more accurate determinations of the mass of the neutron star in three of these systems, i.e. SMC X-1, LMC X-4 and Cen X-3 using the high-resolution Ultraviolet and Visual Echelle Spectrograph UVES on the *Very Large Telescope* (VLT). These systems are in a phase of Roche-lobe overflow, have well determined, circular orbits (P_{orb} of a few days), and an optical counterpart of $V \simeq 14$ mag, i.e. well within reach of VLT/UVES.

Cen X-3 is located in our own galaxy and was identified as the first X-ray pulsar Chodil et al. (1967); Giacconi et al. (1971). The system consists of an O6-7 II-III star (Ash et al. 1999) with a neutron star in a 2.09 day orbit (Nagase et al. 1992). SMC X-1 is located in the Small Magellanic Cloud (SMC). The system hosts a B0.5 Ib supergiant (Hutchings et al. 1977) with a neutron star in a 3.89 day orbit (Nagase et al. 1992). LMC X-4 is located in the Large Magellanic Cloud (LMC) and consists of a $\sim 20 M_{\odot}$ O8 III star (Kaper et al., 2005) and a neutron star in a 1.41 day orbit (Levine et al. 2000).

We have obtained a dozen spectra of all three systems with VLT/UVES in service mode in the period October 2001 to March 2002. The spectra have a resolving power of $\sim 40\,000$, sufficient to measure line positions with an accuracy

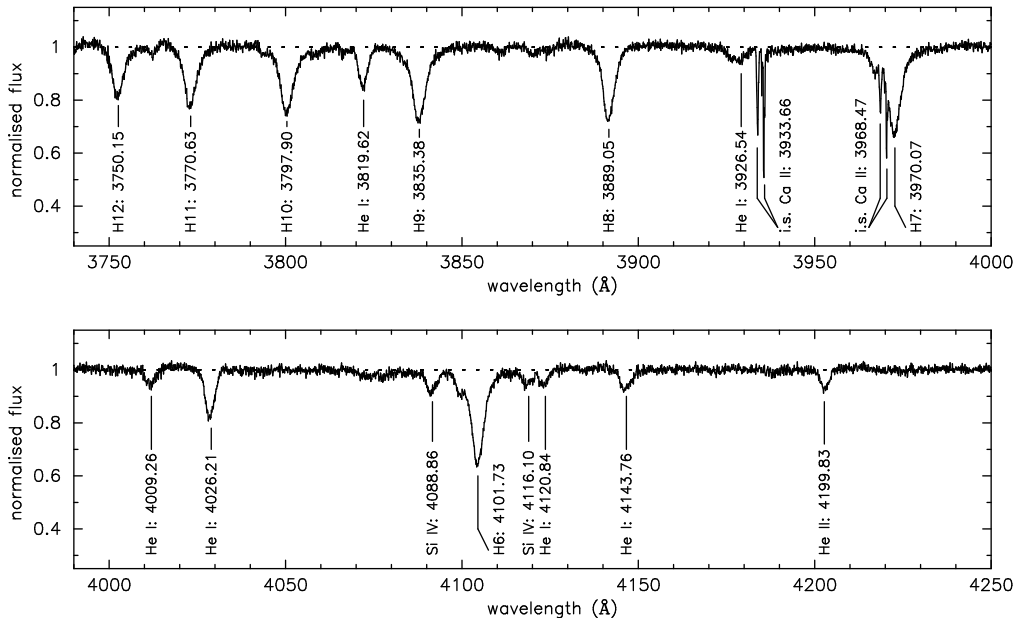


Figure 1. Spectrum of SMC X-1 in the wavelength range 3750–4250 Å, obtained by the blue arm of the UVES spectrograph at orbital phase $\phi \sim 0.51$. Many H and He lines are detected as well as a few metal lines. The spectrum has a $S/N \sim 45$.

of a few km s^{-1} and cover the wavelength range 3600–6600 Å. Figure 1 shows part of the spectrum of SMC X-1. The spectra of LMC X-4 and Cen X-3 are of similar quality. For an extensive description of the full dataset, we refer to Van der Meer et al. (2005).

3. Spectral Analysis

To obtain a radial velocity measurement, often the complete spectra are cross correlated with a template spectrum. In our case the spectra are of such high quality that a radial velocity can be determined for each line separately. The advantage of such a strategy is that it is possible to map the influence of possible distortions due to X-ray heating, gravitational darkening and geometry of the line formation region. Here we select three lines, i.e. H I at 3797.90 Å, He I at 4026.21 Å and He I at 4471.50 Å, that are not affected by the stellar wind and that can be clearly separated from other lines. In Van der Meer et al. (2005) we present a velocity moment analysis to select the lines with objective criteria. To determine the line centre we fit the lines with a gaussian profile. In this way we obtain a radial velocity curve, which we fit with a sinusoidal profile (i.e. a circular orbit).

The X-ray pulsar’s orbital period is accurately known from pulse time delay measurements. To determine the orbital phase of the system we use the ephemeris of Wojdowski et al. (1998), Levine et al. (2000) and Nagase et al. (1992) for SMC X-1, LMC X-4 and Cen X-3, respectively. The orbits are

circular. The fit parameters that remain are the amplitude of the radial velocity curve, K_O , and the γ velocity of the system, v_γ . A few example radial velocity curves are shown in Fig. 2 for the H I line at 3797.90 Å and the He I line at 4471.50 Å.

4. Neutron Star Mass

In order to measure the mass of the neutron star and its optical companion we apply the mass function. For a circular orbit it can be shown that this is defined as:

$$M_X = \frac{K_O^3 P}{2\pi G \sin^3 i} \left(1 + \frac{K_X}{K_O}\right)^2, \quad (1)$$

where M_O and M_X are the mass of the optical component and the X-ray source, respectively, K_O and K_X are the semi-amplitude of the radial velocity curve, P is the period of the orbit and i is the inclination of the orbital plane to the line of sight. The value for K_X and P can be obtained very accurately from X-ray pulse timing delay measurements. Our observations provide a value for K_O . For the determination of the inclination of the system we use the approach of Rappaport & Joss (1983), who showed that:

$$\sin i \approx \frac{\sqrt{1 - \left(\frac{R_L}{a'}\right)^2}}{\cos \theta_e} \quad (2)$$

In this form the equation only holds for an optical component filling its Roche lobe, where R_L is its Roche-lobe radius, a' is the separation of the centres of masses of the two components, and θ_e is the semi-eclipse angle of the compact object. Since in most of these systems soft X-rays are absorbed by the extended stellar wind of the optical companion, the eclipse lasts longer at low energies (see e.g. Haberl et al. 1994; Van der Meer et al. 2004). A more accurate value is obtained from high energy measurements. The ratio of the Roche-lobe radius and the orbital separation can be approximated by:

$$\frac{R_L}{a'} \approx 0.376 - 0.227 \log \frac{K_O}{K_X} - 0.028 \log^2 \frac{K_O}{K_X} \quad (3)$$

The value of the constants were determined by Rappaport & Joss (1983). These depend on the ratio of the rotational period of the optical companion and the orbital period of the system. For a system undergoing Roche-lobe overflow, i.e. the system is tidally locked, one can assume that this ratio equals 1. This can be verified by determining the rotational period of the optical companion separately by measuring its (projected) rotational velocity.

Using the formulas above we determine the mass of the neutron stars in our sample. The results and literature values are listed in Table 1.

5. Conclusions

We show that with our VLT/UVES observations the mass measurements of the neutron stars in HMXBs are significantly improved. The masses are not all

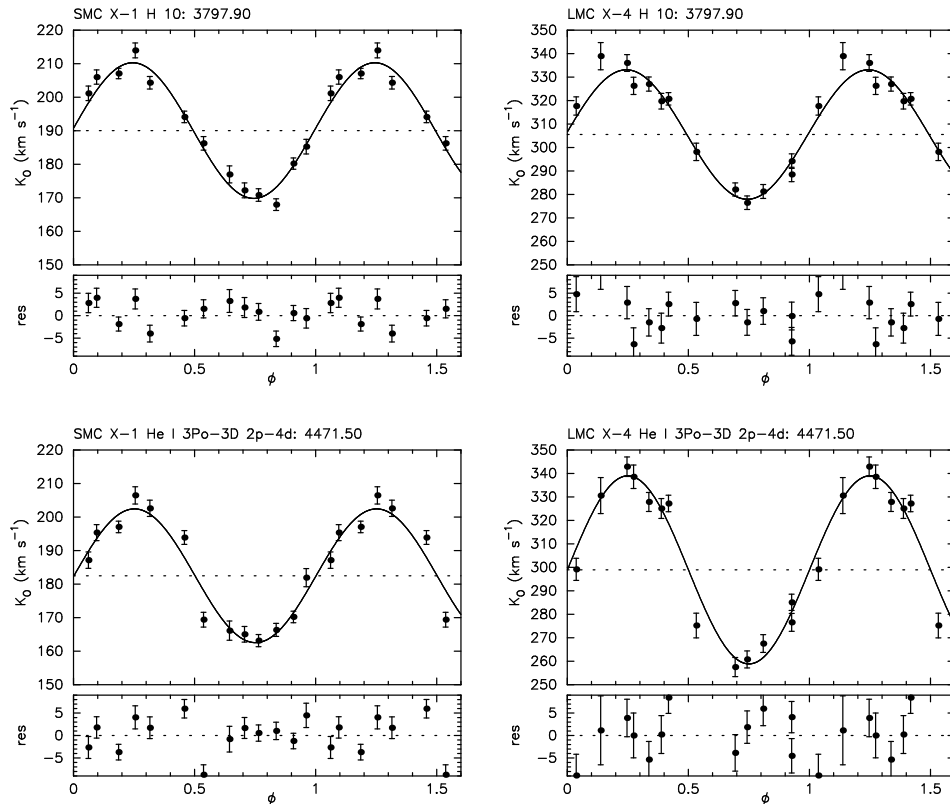


Figure 2. For each selected line that is clearly separated, that has a unique identification and is not affected by the stellar wind of the OB-supergiant a radial velocity can be determined. Here the velocity amplitudes of the H I line at 3797.90 Å and the He I line at 4471.50 Å with their fitted radial velocity curve is shown for SMC X-1 and LMC X-4. The lower panels show the residuals of the fit to the datapoints.

higher than $1.4 M_{\odot}$, as is the case for Vela X-1. The mass of SMC X-1, which is $1.05 \pm 0.09 M_{\odot}$, is actually the lowest neutron star mass measured so far. Therefore, we conclude that a mass distribution of neutron stars is present in HMXBs. Possible distortions by gravitational darkening and X-ray heating, that can influence the value of the radial velocity amplitude of the optical companion, are discussed in Van der Meer et al. (2005).

The most accurate neutron star masses have been derived for the binary radio pulsars. Thorsett & Chakrabarty (1999) showed that most of these pulsars have a mass that is consistent with a small range near $1.35 M_{\odot}$. Currently, the sample contains more systems and it is clear that a broader range from $1.25 - 1.44 M_{\odot}$ exists (Stairs 2004). Van den Heuvel (2004) suggests that the secondary formed neutron star in these systems tends to be the less massive of the two. On the other hand, our result shows that the primary formed neutron star can have a low mass as well. A mass distribution of neutron stars in binary radio pulsars as well as in HMXBs sets an important constraint on the formation mechanism of neutron stars.

Table 1. List of all the parameters obtained from literature. All errors are 1σ .

system	P (days)	$a_x \sin i$ (lt s)	Θ_e	\bar{K}_X (km s $^{-1}$)
SMC X-1	3.89229090(43)	53.4876(4)	29 ± 2	299.595 ± 0.002
LMC X-4	1.40839776(26)	26.343(16)	27 ± 3	407.8 ± 0.3
Cen X-3	2.08713845(5)	39.56(7)	34 ± 3	413.2 ± 0.7

system	\bar{K}_O (km s $^{-1}$)	i ($^\circ$)	M_O (M_\odot)	M_X (M_\odot)
SMC X-1	20.3 ± 0.9	68 ± 3	15.5 ± 1.5	1.05 ± 0.09
LMC X-4	34.3 ± 1.2	65 ± 4	15.6 ± 1.8	1.31 ± 0.14
Cen X-3	26.0 ± 2.5	73 ± 10	19.7 ± 4.3	1.24 ± 0.24

References

- Ash, T. D. C., Reynolds, A. P., Roche, P., Norton, A. J., Still, M. D., & Morales-Rueda, L. 1999, *MNRAS*, 307, 357
- Barziv, O., Kaper, L., Van Kerkwijk, M. H., Telting, J. H., & Van Paradijs, J. 2001, *A&A*, 377, 925
- Brown, G. E., & Bethe, H. A. 1994, *ApJ*, 423, 659
- Burrows, A. 2000, *Nat*, 403, 727
- Chodil, G., Mark, H., Rodrigues, R., Seward, F., Swift, C. D., Hiltner, W. A., Wallerstein, G., & Mannery, E. J. 1967, *Physical Review Letters*, 19, 681
- Giacconi, R., Gursky, H., Kellogg, E., Schreier, E., & Tananbaum, H. 1971, *ApJ*, 167, L67+
- Haberl, F., Aoki, T., & Mavromatakis, F. 1994, *A&A*, 288, 796
- Hutchings, J. B., Cowley, A. P., Osmer, P. S., & Crampton, D. 1977, *ApJ*, 217, 186
- Lattimer, J. M., & Prakash, M. 2004, *Science*, 304, 536
- Levine, A. M., Rappaport, S. A., & Zojcheski, G. 2000, *ApJ*, 541, 194
- Nagase, F., Corbet, R. H. D., Day, C. S. R., Inoue, H., Takeshima, T., Yoshida, K., & Mihara, T. 1992, *ApJ*, 396, 147
- Quaintrell, H., Norton, A. J., Ash, T. D. C., Roche, P., Willems, B., Bedding, T. R., Baldry, I. K., & Fender, R. P. 2003, *A&A*, 401, 313
- Rappaport, S. A., & Joss, P. C. 1983, in *Accretion-Driven Stellar X-ray Sources*, 1-39
- Srinivasan, G. 2001, in *Black Holes in Binaries and Galactic Nuclei*, 45-+
- Stairs, I. H. 2004, *Science*, 304, 547
- Thorsett, S. E., & Chakrabarty, D. 1999, *ApJ*, 512, 288
- Timmes, F. X., Woosley, S. E., & Weaver, T. A. 1996, *ApJ*, 457, 834
- Van den Heuvel, E. P. J. 2004, *astro-ph/0407451*
- Van der Meer, A., Kaper, L., Di Salvo, T., Méndez, M., Van der Klis, M., Barr, P., & Trams, N. R. 2004, *astro-ph/0412021*
- Van Kerkwijk, M. H., Van Paradijs, J., & Zuiderwijk, E. J. 1995, *A&A*, 303, 497
- Wojdowski, P., Clark, G. W., Levine, A. M., Woo, J. W., & Zhang, S. N. 1998, *ApJ*, 502, 253